

# An Environmental-Sensitive BODIPY<sup>®</sup>-Derivative with Bioapplication: Spectral and Photophysical Properties

Mikael Isaksson,<sup>1</sup> Stanislav Kalinin,<sup>1</sup> Sergei Lobov,<sup>2</sup> Tor Ny,<sup>2</sup>  
and Lennart B.-Å. Johansson<sup>1,3</sup>

Received March 28, 2003; revised May 7, 2003; accepted May 7, 2003

A previously synthesised derivative of BODIPY aimed for sulfhydryl specific labelling of cysteine residues in proteins was studied. The spectral and photophysical properties of this derivative, *N*-(4,4-difluoro-1,3,5,7-tetramethyl-4-bora-3a,4a-diaza-*s*-indacene-2-yl) iodoacetamide (NBDY) were characterised, and found to be considerably different from those of commonly used derivatives of BODIPY, e.g. *N*-(4,4-difluoro-5,7-dimethyl-4-bora-3a,4a-diaza-*s*-indacene-3-yl)methyl iodoacetamide. The absorption and fluorescence spectra, as well as fluorescence lifetimes and quantum yields of NBDY are quite sensitive to solvent properties. The fluorescence is effectively quenched by I<sup>-</sup> when NBDY is free in water or attached to Cys in different mutants of plasminogen activator inhibitor type 2 (PAI-2). A ground-state dimer forms when two NBDY groups are closely spaced in plasminogen activator inhibitor type 1 (PAI-1).

**KEY WORDS:** BODIPY; donor–donor energy migration; homotransfer; dimers; quenching.

## INTRODUCTION

Spectral and photophysical properties of frequently used derivatives of BODIPY<sup>®</sup> like *N*-(4,4-difluoro-1,3,5,7-tetramethyl-4-bora-3a,4a-diaza-*s*-indacene-2-yl) iodoacetamide and *N*-(4,4-difluoro-5,7-dimethyl-4-bora-3a,4a-diaza-*s*-indacene-3-yl) methyl iodoacetamide (SBDY, see Fig. 1) exhibit extraordinary stability to various physico-chemical environments [1]. The explanation is ascribed to the small change in permanent dipole moment upon excitation, as well as the fact the permanent dipole and electronic ( $S_0 \leftrightarrow S_1$ ) transition dipoles are perpendicular [2]. SBDY is a sulfhydryl specific reagent [3], which for several years has been used for labelling cysteine residues in proteins. As was previously demonstrated the photophysical properties

of SBDY make it suitable for distance measurements based on donor-donor energy migration (DDEM) [4–7]. In applications of the DDEM method [8], chemically and photophysically identical fluorescent groups are incorporated at well-defined positions in a biomacromolecule, e.g. a protein. For such a system the rate of energy migration can be obtained only from analyses of fluorescence depolarisation measurements, since the rate of fluorescence relaxation remains invariant to energy migration. However, this statement is not true for pairs of chemically identical but photophysically non-identical fluorescent groups. The photophysics' decay of such pairs contains information about the energy migration/transfer rates, and thus about the distance between interacting molecules within the pair. To distinguish from DDEM, we hereafter refer to the latter case as partial donor-donor energy migration (PDDEM). In a recent paper [9] the theory and applicability of PDDEM was outlined, and later applied on lipid membranes [10] and protein systems [Unpublished results].

For PDDEM experiments on proteins, NBDY renders particular interest among different BODIPY derivatives,

<sup>1</sup> Department of Chemistry; Biophysical Chemistry, Umeå University, S-901 87 Umeå, Sweden.

<sup>2</sup> Department of Medical Biochemistry and Biophysics, Umeå University, S-901 87 Umeå, Sweden.

<sup>3</sup> To whom correspondence should be addressed. E-mail: lennart.johansson@chem.umu.se

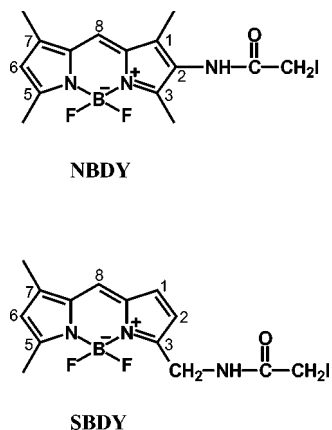


**Fig. 1.** Chemical structures of *N*-(4,4-difluoro-1,3,5,7-tetramethyl-4-bora-3a,4a-diaza-*s*-indacene-2-yl)iodoacetamide (NBDY) and *N*-(4,4-difluoro-5,7-dimethyl-4-bora-3a,4a-diaza-*s*-indacene-3-yl)methyl iodoacetamide (SBDY).

which is here supported by studies of NBDY dissolved in solvents of different polarity, as well as specifically attached to different positions in a protein. The proteins used in most experiments were different mutants of plasminogen activator inhibitor type 2 (PAI-2) [11]. Mutants of plasminogen activator inhibitor type 1 (PAI-1) were used to study ground state dimerisation of NBDY. PAI-1 and PAI-2 belong to the large and diverse family of serine proteinase inhibitors (serpins) that encompasses a wide range of proteins, mostly proteinase inhibitors [12], which are widely distributed in eukaryotes and control all the major proteolytic cascades in humans.

## MATERIALS AND METHODS

*N*-(4,4-difluoro-1,3,5,7-tetramethyl-4-bora-3a,4a-diaza-*s*-indacene-2-yl) iodoacetamid (BODIPY<sup>®</sup> 507/545 IA; NBDY) was purchased from Molecular Probes, Inc. (USA), glass distilled glycerol was from OmniSolv (USA). All chemicals used were of analytical grade.

NBDY derivative of 2-mercaptoethanol was prepared as follows. NBDY iodoacetamide dissolved in DMSO was treated with the excess of 2-mercaptoethanol (5% in 20mM Tris-HCl aqueous buffer, pH 7.4). The product was purified by TLC (Silica gel 60 plates, Merck, Germany) by using the solvent mixture of chloroform-methanol-water (by volume 90 : 10 : 0.1,  $R_f \sim 0.4$ ).

### Preparation and Labelling of PAI-1 and PAI-2 Mutants

PAI-2 mutagenesis, expression and purification were done as described previously [13]. PAI-2 mutants (Table I)

**Table I.** Notation Used for Referring to Different Substitution Mutants of Plasminogen Activator Inhibitor Type 2 (PAI-2)

Shorthand notation	Substitutions
79cysPAI-2	C5S/C145S/C161S/C405S
161cysPAI-2	C5S/C79S/C145S/C405S
171cysPAI-2	C5S/C79S/C145S/C161S/S171C/C405S
347cysPAI-2	C5S/C79S/C145S/C161S/N347C/C405S

were labelled and purified further as described in Lobov *et al.* [14].

The construction of PAI-1 Cys-double mutant S344C-M347C was described previously [15]. The inhibitor activity was determined by a chromogenic assay and by complex formation with urokinase type plasminogen activator (uPA) [16]. Labelling of the double mutant S344C-M347C was performed as described elsewhere [6], with the exception that the probe was NBDY and Tween was omitted from the chromatography buffer. Samples were studied in both the absence and presence of glycerol (50% w/w).

*Absorption spectra* were measured on a GBC 920 spectrophotometer (GBC, Australia). Steady-state fluorescence spectra were recorded on a SPEX Fluorolog 112 (SPEX, USA) and a SPEX Fluorolog-3 (SPEX, USA) instrument both equipped with Glan-Thompson polarisers. The spectral bandwidths were typically set to 5.5 and 3.6 nm and 2.0 and 2.0 nm for the excitation and emission monochromators, respectively. All spectra were corrected.

*Time-correlated single-photon-counting measurements* were performed using a PRA 3000 (PRA, Canada) system. The excitation source was a NanoLED-01 (IBH, Scotland) pulsed diode, operated at 800 kHz. The excitation and emission wavelengths were selected using interference filters (Melles Griot, the Netherlands) centred at 500 and 550 nm. The fluorescence decays were collected over 1024 channels with the resolution of 50 ps/ch, with at least 10 000 photons in the peak-maximum.

All measurements were performed at room temperature except for the steady-state anisotropy measurements that were performed at 277 K. The maximum absorbance of all samples was kept below 0.08.

*Fluorescence quantum yields* were measured when using a perylene dye dissolved in chloroform [17] and tetramethyl-BODIPY in methanol as quantum yield standards. The quantum yields of these compounds are 1.0 [17] and 0.93 [1], respectively.

The Förster radius ( $R_0$ ) of donor-donor energy transfer [17] was calculated according to

$$R_0 = \left( \frac{9000 \ln 10 (2/3) \Phi J}{128 \pi^5 n^4 N_A} \right)^{1/6} \quad (1)$$

where  $N_A$ ,  $n$  and  $\Phi$  denote the Avogadro constant, the refractive index of the medium and the quantum yield of the donor, respectively. The overlap integral  $J$  is given by

$$J = \int \varepsilon(v)F(v)v^{-4} dv \quad (2)$$

In eq. 2,  $v$  and  $\varepsilon(v)$  denote the wavenumber and the molar absorptivity, respectively. The corrected emission spectrum  $F(v)$  is normalised so that  $\int F(v) dv = 1$ .

The radiative lifetimes ( $\tau_0$ ) were calculated according to the Strickler-Berg equation [18]

$$\frac{1}{\tau_0} = 2.88 \times 10^{-9} n^2 \frac{\int F(v)dv}{\int F(v)v^{-3}dv} \int \varepsilon(v)v^{-1}dv \quad (3)$$

In the fluorescence quenching experiments small aliquots of KI were added to the sample, thereafter the fluorescence intensity was integrated over the emission peak.  $\text{Na}_2\text{S}_2\text{O}_3$  was added to avoid formation of  $\text{I}_2$ . The data was analysed by standard Stern-Volmer analysis [19] according to the equation

$$\frac{F_0}{F} = 1 + k_q \tau_0 [Q] = 1 + K_D [Q] \quad (4)$$

Eq. 4 accounts for dynamic quenching where  $[Q]$  denotes the concentration of quencher,  $F_0$  and  $F$  are the fluorescence intensities in the absence and presence of quencher. The lifetime  $\tau_0$  is here defined as the lifetime in absence of quencher and  $k_q$  is the bimolecular quenching constant. For diffusion controlled quenching  $k_q$  is typically about  $10^{10} \text{ M}^{-1} \text{ s}^{-1}$ . Slower rates can be expected when the probe is partly shielded from the quencher.

For probes attached to proteins a modified Stern-Volmer plot was used [19].

$$\frac{F_0}{\Delta F} = \frac{1}{f_a K_a} \cdot \frac{1}{[Q]} + \frac{1}{f_a} \quad (5)$$

Here it is assumed that a fraction ( $f_a$ ) of the probes is accessible to quenchers.  $K_a$  is the Stern-Volmer quenching constant for the accessible part.

## RESULTS AND DISCUSSION

Spectral and photophysical properties of *N*-(4,4-difluoro-1,3,5,7-tetramethyl-4-bora-3a,4a-diaza-*s*-indacene-2-yl) iodoacetamid (NBDY, see Fig. 1) were determined for the probe dissolved in water, organic solvents, and covalently attached to Cys residues in plasminogen activator inhibitor type 2 (PAI-2). Throughout this paper NBDY is compared to *N*-(4,4-difluoro-5,7-dimethyl-4-bora-3a,4a-diaza-*s*-indacene-3-yl) methyl iodoacetamid (SBDY, see Fig. 1), which exhibit properties commonly found for numerous derivatives of BODIPY.

### Absorption and Fluorescence Spectra

Absorption spectra of NBDY in chloroform, methanol and acetonitril are very similar, while spectral shifts and broadening are observed in DMSO and water (Table II, Fig. (2A)). Moreover the spectra recorded for NBDY dissolved in water are very similar to those obtained for NBDY attached to different Cys residues of PAI-2. This finding is compatible with a probe location in the water-protein interface.

**Table II.** Absorption and Steady-State Fluorescence Properties of NBDY in Different Solvents, as well as Covalently Linked to Different Mutant Forms of PAI-2

NBDY	$\lambda_{\text{max}}$ (nm)	$\varepsilon_{\text{max}}$ ( $\text{M}^{-1} \text{ cm}^{-1}$ )	$\lambda_{\text{em}}$ (nm)	Stokes' shift (nm)	$\Phi$	$R_0$ (Å)
Chloroform	513	82800	549	36	$0.73 \pm 0.04$	$42.5 \pm 0.8$
MeOH	508	84200	549	41	$0.34 \pm 0.02$	$36.6 \pm 0.7$
EtOH	509	84100	552	43	$0.38 \pm 0.02$	$36.5 \pm 0.7$
Acetonitrile	507	77400	554	47	$0.30 \pm 0.02$	$34.1 \pm 0.7$
DMSO	512	69000	563	51	$0.26 \pm 0.02$	$30.3 \pm 0.8$
Water	504	74400	533	29	$0.33 \pm 0.02$	$37.4 \pm 0.7$
347cys PAI-2 <sup>a</sup>	508	69000	537	29	$0.63 \pm 0.05$	$44.9 \pm 1$
79cys PAI-2 <sup>a</sup>	509	69000	537	28	$0.62 \pm 0.05$	$45.3 \pm 1$
171cys PAI-2 <sup>a</sup>	509	69000	538	29	$0.43 \pm 0.05$	$39.7 \pm 1$
161cys PAI-2 <sup>a</sup>	509	69000	538	29	$0.36 \pm 0.05$	$42.2 \pm 1$
79cys PAI-2 <sup>b</sup>	510	69000	537	27	$0.38 \pm 0.05$	$41.9 \pm 1$
347cys PAI-2 <sup>b</sup>	508	69000	529	21	$0.38 \pm 0.05$	$42.4 \pm 1$

*Note.* The fluorescence quantum yield and the Förster radius are denoted  $\Phi$  and  $R_0$ , respectively.

<sup>a</sup>Dissolved in a glycerol:Tris-aqueous buffer (50% w/w).

<sup>b</sup>Dissolved in Tris-aqueous buffer.

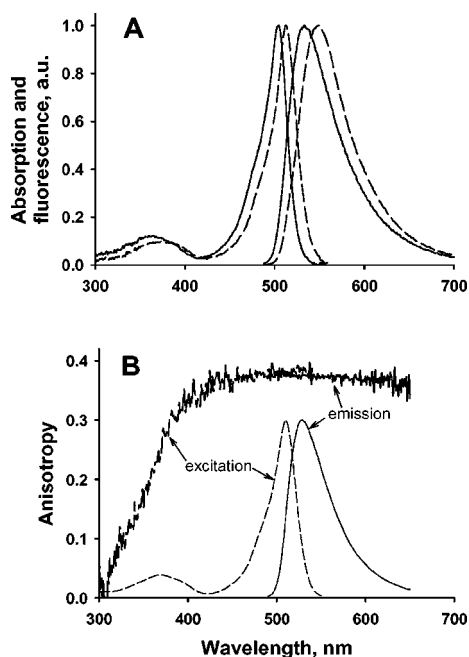


**Fig. 2.** A: Normalised absorption and emission spectra of NBDY (reacted with 2-mercaptoethanol, See Materials and Methods) in pure water (solid lines) and in chloroform (dashed lines). B: Excitation (dashed line) and emission (solid line) anisotropy spectra of NBDY in glycerol at 277 K. The excitation and emission spectra are also shown. The NBDY concentrations were 0.5–0.6  $\mu\text{M}$ .

Fluorescence spectra of NBDY exhibit maximum and minimum Stokes' shift of 51 and 29 nm for DMSO and water, respectively. The corresponding shifts for SBDY are typically about 5 nm. Unlike SBDY the fluorescence and absorption spectra of NBDY deviate much from mirror images. The reason is likely due to orbital contact between the *N*-atom of the amide group and C2-atom of the BODIPY core. Hereby the electronic distribution of the BODIPY core becomes more sensitive to *e.g.* hydrogen bonding to the amide group. Moreover the permanent electric dipole and the  $S_0 \leftrightarrow S_1$  transition dipole moments are likely no longer perpendicular. Recent studies of BODIPY derivatives in which a phenyl or an etynylphenyl group is bound to C2 reveal similar spectral changes [20].

### Fluorescence Anisotropy

To characterise the electronic transitions, the fluorescence excitation and emission anisotropies of NBDY in glycerol were determined. By cooling, the rotational motions of NBDY were immobilised on the timescale of fluorescence. Hence, the anisotropy data displayed in Fig 2(B) represent limiting anisotropies. The excitation anisotropy shows that the main absorption band ( $S_0 \rightarrow S_1$  transi-

tion) is a pure electronic transition, while the second weak transition located at about 360 nm is mixed. Because the 360 nm band is weak, it might contain intensity-borrowing from higher electronic states. Such transitions typically show a wavelength dependent excitation anisotropy. The limiting anisotropy value of the  $S_0 \rightarrow S_1$  transition is 0.37, which is similar to that found for SBDY and related derivatives of BODIPY [1].

### Fluorescence Quantum Yields and Lifetimes

Fluorescence quantum yields and lifetimes obtained for NBDY in different solvents and in different positions of PAI-2 are summarised in Tables II and III. The fluorescence relaxation is a single exponential decay in all solvents studied, while bi-exponential fits are needed for the mutant forms of PAI-2. Lifetimes and quantum yield are strongly dependent on the solvent properties, as is expected since spectra of NBDY also exhibit solvent dependence (See above). The quantum yields and average lifetimes of NBDY in PAI-2 dissolved in water are similar to those of free NBDY in water, which is compatible with their location in the protein structure. From the ratio between measured lifetimes and quantum yields the radiative lifetimes were calculated. The values obtained are displayed in Table III together with the values calculated by using the Strickler-Berg equation [18]. Throughout we find that the calculated radiative lifetimes are shorter than those obtained from lifetime and quantum yield measurements. This can be expected because of lacking mirror

**Table III.** The Radiative ( $\tau_0$ ) and Experimental ( $\tau$ ) Fluorescence Lifetimes of NBDY in Different Solvents, as well as Covalently Linked to Different Mutant Forms of PAI-2

Solvent	$\tau$ (ns)	$\tau_0$ (ns) <sup>d</sup>	$\tau/\Phi$ (ns)
Chloroform	4.6 $\pm$ 0.1	4.7 $\pm$ 0.3	6.3 $\pm$ 0.7
MeOH	2.8 $\pm$ 0.1	5.7 $\pm$ 0.3	8.2 $\pm$ 0.9
EtOH	3.0 $\pm$ 0.1	5.4 $\pm$ 0.3	7.9 $\pm$ 0.8
Acetonitrile	2.7 $\pm$ 0.1	5.7 $\pm$ 0.4	9.2 $\pm$ 0.8
DMSO	2.1 $\pm$ 0.1	4.5 $\pm$ 0.6	8.1 $\pm$ 1.1
Water	2.6 $\pm$ 0.1	5.2 $\pm$ 0.4	7.8 $\pm$ 0.9
347cys PAI-2 <sup>a</sup>	4.0 $\pm$ 0.1 <sup>c</sup>	5.3 $\pm$ 0.5	6.3 $\pm$ 1.0
79cys PAI-2 <sup>a</sup>	4.1 $\pm$ 0.1 <sup>c</sup>	5.3 $\pm$ 0.5	6.6 $\pm$ 1.0
171cys PAI-2 <sup>a</sup>	3.5 $\pm$ 0.1 <sup>c</sup>	5.4 $\pm$ 0.5	8.2 $\pm$ 1.0
161cys PAI-2 <sup>a</sup>	3.5 $\pm$ 0.1 <sup>c</sup>	5.3 $\pm$ 0.5	9.6 $\pm$ 1.0
79cys PAI-2 <sup>b</sup>	4.0 $\pm$ 0.1 <sup>c</sup>	5.4 $\pm$ 0.3	10.5 $\pm$ 1.0
347cys PAI-2 <sup>b</sup>	3.9 $\pm$ 0.1 <sup>c</sup>	5.9 $\pm$ 0.5	10.2 $\pm$ 1.0

<sup>a</sup>Dissolved in a glycerol: Tris-aqueous buffer (50% w/w).

<sup>b</sup>Dissolved in Tris-aqueous buffer.

<sup>c</sup>Average lifetime, calculated from a bi-exponential fit  $F(t) = a_1 \exp(-t/\tau_1) + a_2 \exp(-t/\tau_2)$ , from which the average lifetime is given by  $\langle \tau \rangle = \{a_1(\tau_1)^2 + a_2(\tau_2)^2\} / \{a_1\tau_1 + a_2\tau_2\}$ .

<sup>d</sup>Calculated using the Strickler-Berg equation [18].

image symmetry between absorption and corrected fluorescence spectra.

### Fluorescence Quenching

For PDDEM experiments with proteins it is of interest to achieve different fluorescence lifetimes of fluorescent groups located in different positions of the structure. In the experiments of NBDY in various mutants of PAI-2 the quenching by acrylamide and  $I^-$  was examined. The quenching by  $I^-$  was much more efficient than that of acrylamide for all PAI-2 mutants studied. The surface charge, as well as spatial accessibility of the protein may significantly regulate the quenching efficiency by  $I^-$ . In Fig. 3 a standard Stern-Volmer plot of  $F_0/F$  vs.  $I^-$ -concentration, is displayed for NBDY covalently attached to the Cys171 residue of 171cys PAI-2. The plot reveals a negative curvature with increasing quencher concentration, indicating a sterical shielding of the NBDY-group. However plotting  $F_0/\Delta F$  vs.  $1/[I^-]$  (see Material and Methods) gives a straight line with a coefficient of determination (or the square of the correlation coefficient) being 0.999. Although minor deviations from linearity might be seen at low concentrations these could be ascribed to relative errors in the titration volumes (*i.e.* larger errors for smaller volumes). A linear  $F_0/\Delta F$  vs.  $1/[I^-]$  graph is compatible with “a two-state model” that assumes the existence of two types of probe populations inside the protein, one accessible to the quencher and the other shielded from it [19]. As can be seen from Table IV, the quenching rates by  $I^-$  vary as much as a factor of two between different labelling positions. The fact that different sites expose

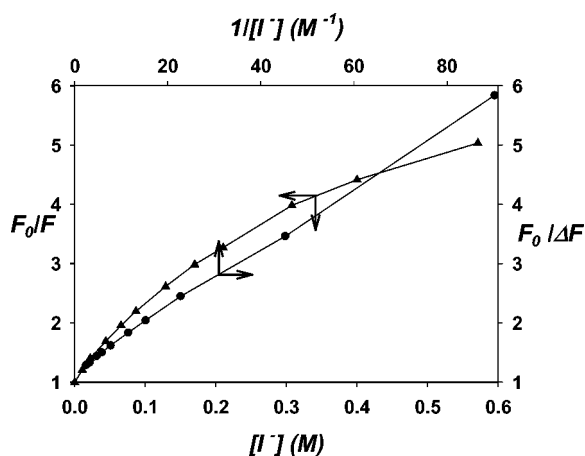


Fig. 3. Standard Stern-Volmer plot (▲) and modified Stern-Volmer plot (●) of NBDY-labelled 171cys PAI-2 mutant in water buffer quenched by KI.

Table IV. Quenching Properties of NBDY Attached to Different Cys Residues of PAI-2 Mutants Dissolved in Water Buffer. For a Comparison, Free NBDY Dissolved in Water Buffer was Also Studied

NBDY	$k_q$ ( $M^{-1} ns^{-1}$ )	$f_a$	$K_D$ ( $M^{-1}$ )
79cys PAI-2	3.6	0.63	14.5
347cys PAI-2	2.4	0.96	9.4
171cys PAI-2	6.7	0.83	23.6
Water buffer	11.0	1.0	28.6

different fractions of available probes to quenchers provides opportunity to control the fluorescence quenching in various parts of a protein. For this purpose,  $I^-$  is an efficient water-soluble quencher with typical quenching rates  $k_q \approx 10^{10} M^{-1} s^{-1}$ , *i.e.* close to the diffusion-controlled limit.

One should notice that the emission spectra of the quenched systems are not shifted as compared to those of the unquenched systems. The absorption spectra exhibit only a minor red shift. The steady-state fluorescence anisotropy was determined as the  $I^-$ -concentration was increased up to 0.5 M. The anisotropy increased from 0.24 to 0.33, as is expected because the average fluorescence lifetimes decrease with increasing concentration.

### Förster Radii

As can be expected, the Förster radii ( $R_0$ ) of NBDY differ between various systems. This is explained by the change of spectral and photophysical properties with different local environment. For different solvents the influence on  $R_0$  is quite substantial with values ranging from about 30 to 42 Å, as is shown in Table II. These  $R_0$ -values are lower than the value of  $R_0 = 57 \pm 1 \text{ Å}$  found for SBDY and related compounds [1]. For NBDY attached to different Cys mutants of PAI-2 dissolved in water, the Förster radii are typically about 42 Å.

### Dimerisation

NBDY can form dimers as is here shown by labelling adjacent positions in PAI-1. We studied doubly NBDY-labeled Cys mutants of active PAI-1 (S344C and M347C, see Materials and Methods). Upon reaction with the urokinase-type plasminogen activator (uPA), the reactive centre loop is cleaved between residues 346 and 347. This is followed by a major translocation of one end of the loop resulting in a distance between the two mutated residues of about 60 Å [7]. In active PAI-1 the absorption spectrum is a mixture of the monomer and the

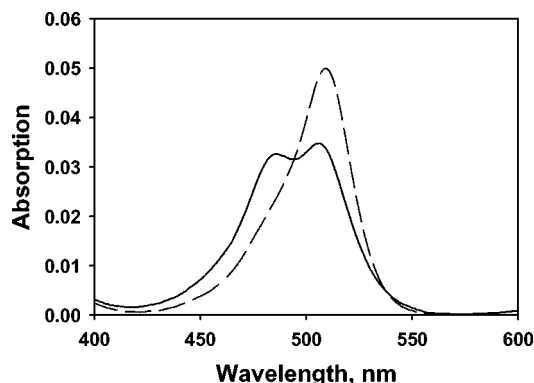


**Fig. 4.** Absorption spectra of the double mutant S344C-M347C of PAI-1 labelled with NBDY before (solid line) and after (dashed line) cleavage of the reactive centre loop. The spectra were measured in glycerol-water buffer (50% w/w) at 277 K. The NBDY concentrations were 0.75  $\mu$ M.

dimer spectra, while the spectrum in the cleaved form shows a pure monomer spectrum (Fig. 4). The dimers exhibit a blue-shifted absorption spectrum relative to that of the monomer. No detectable dimer-fluorescence was observed. Recent experiments have revealed that SBDY and similar derivatives of BODIPY may form ground-state dimers [2,21].

### Photostability

The fluorescence spectra and intensities of SBDY remain invariant to the excitation light exposure under typical experimental conditions, as is the case in present study (*cf.* Materials and Methods). The fluorescence of NBDY, however, undergoes irreversible photobleaching in the protein as well as solvents. To avoid this, spectral bandwidths and exposure times were decreased. The bleaching of NBDY in PAI-2 is somewhat faster as compared to that of NBDY dissolved in ethanol. Thus in using NBDY it is highly recommended always to be careful in choosing the proper experimental conditions.

### CONCLUSIONS

*N*-(4,4-difluoro-1,3,5,7-tetramethyl-4-bora-3a,4a-diaza-*s*-indacene-2-yl) iodoacetamid (BODIPY<sup>®</sup> 507/545 IA; NBDY) exhibit more complex light spectroscopic properties as compared to most BODIPY derivatives frequently used in applications. Fluorescence quantum yield, lifetime as well as spectra are sensitive to the local polarity of the NBDY group. The different quenching of NBDY localised in different sites of a protein makes it suitable for PDDEM applications. Moreover the shorter Förster radius ( $\approx 42$  Å) as compared to that of SBDY

means that it can be used to measure shorter distances in proteins. It is also worth noticing that NBDY in proteins can form a non-fluorescent ground state dimer. Finally, particular care in light exposure of NBDY is recommended.

### ACKNOWLEDGMENT

The Swedish Research Council, the Kempe Foundations and a Biotechnical Grant from Umeå University have financially supported this work.

### REFERENCES

1. J. Karolin, L. B.-Å. Johansson, L. Strandberg, and T. Ny (1994). *J. Am. Chem. Soc.* **116**(17), 7801–7806.
2. F. Bergström, I. Mikhalyov, P. Hägglöf, R. Wortmann, T. Ny, and L. B.-Å. Johansson (2002). *J. Am. Chem. Soc.* **124**, 196–204.
3. R. P. Haugland. (1996). *Handbook of Fluorescent Probes and Research Chemicals*, 6th ed., Molecular Probes, Inc., Eugene, OR.
4. J. Karolin, M. Fa, M. Wilczynska, T. Ny, and L. B.-Å. Johansson (1998). *Biophys. J.* **74**, 11–21.
5. F. Bergström, P. Hägglöf, J. Karolin, T. Ny, and L. B.-Å. Johansson (1999). *Proc. Natl. Acad. Sci.* **96**(22), 12477–12481.
6. M. Fa, F. Bergström, P. Hägglöf, M. Wilczynska, L. B.-Å. Johansson, and T. Ny (2000). *Structure* **8**(4), 397–405.
7. M. Wilczynska, M. Fa, J. Karolin, P.-I. Ohlsson, L. B.-Å. Johansson, and T. Ny (1997). *Nat. Struct. Biol.* **4**(5), 354–356.
8. L. B.-Å. Johansson, F. Bergström, P. Edman, I. V. Grechishnikova, and J. G. Molotkovsky (1996). *J. Chem. Soc., Faraday Trans.* **92**(9), 1563–1567.
9. S. V. Kalinin, J. G. Molotkovsky, and L. B.-Å. Johansson (2002). *Spectrochim. Acta Part A* **58**, 1087–1097.
10. S. Kalinin, J. G. Molotkovsky, and L. B.-Å. Johansson (2003). *J. Phys. Chem. B* **107**, 3318–3324.
11. T. Kawano, K. Morimoto, and Y. Uemura (1970). *J. Biochem. (Tokyo)* **67**, 333–342.
12. G. A. Silverman, P. I. Bird, R. W. Carrell, F. C. Church, P. B. Coughlin, P. G. Gettins, J. A. Irving, D. A. Lomas, C. J. Luke, R. W. Moyer, P. A. Pemberton, E. Remold-O'Donnell, G. S. Salvesen, J. Travis, and J. C. Whisstock (2001). *J. Biol. Chem.* **276**, 33293–33296.
13. M. Wilczynska, S. Lobov, and T. Ny (2003). *FEBS Lett* **537**, 11–16.
14. S. Lobov, M. Wilczynska, F. Bergström, L. B.-Å. Johansson, and T. Ny (in press).
15. S. B. Aleshkov, M. Fa, J. Karolin, L. Strandberg, L. B.-Å. Johansson, M. Wilczynska, and T. Ny (1996). *J. Biol. Chem.* **271**(35), 21231–21238.
16. D. Lawrence, L. Strandberg, T. Grundström, and T. Ny (1989). *Eur. J. Biochem.* **186**, 523–533.
17. S. Kalinin, M. Speckbacher, H. Langhals, and L. B.-Å. Johansson (2001). *Phys. Chem. Chem. Phys.* **3**, 172–174.
18. J. B. Birks (1970). *Photophysics of Aromatic Molecules*, Wiley, London.
19. J. R. Lakowicz (1999). *Principles of Fluorescence Spectroscopy*, 2nd ed., Kluwer Academic, New York.
20. C.-W. Wan, A. Burghart, J. Chen, F. Bergström, L. B.-Å. Johansson, M. F. Wolford, T. G. Kim, M. R. Topp, R. M. Hochstrasser, and K. Burgess (in press). *Eur. J. Chem.*
21. I. Mikhalyov, N. Gretskeya, F. Bergström, and L. B.-Å. Johansson (2002). *Phys. Chem. Chem. Phys.* **4**, 5663–5670.